

## Chemical fracture statistics and universal distribution of extreme values

A. BALDASSARRI<sup>1,2,3</sup>, A. GABRIELLI<sup>1,3</sup> and B. SAPOVAL<sup>1,2</sup>

<sup>1</sup> *Laboratoire de Physique de la Matière Condensée, Ecole Polytechnique  
91128 Palaiseau, France*

<sup>2</sup> *CMLA, Ecole Normale Supérieure - 94235 Cachan, France*

<sup>3</sup> *INFN, Dipartimento di Fisica, Università di Roma “La Sapienza”  
P.le A. Moro, 2, I-00185 Roma, Italy*

(received 11 September 2001; accepted in final form 23 April 2002)

PACS. 64.60.Ak – Renormalization-group, fractal, and percolation studies of phase transitions.

PACS. 81.40.Np – Fatigue, corrosion fatigue, embrittlement, cracking, fracture and failure.

**Abstract.** – When a corrosive solution reaches the limits of a solid sample, a chemical fracture occurs. An analytical theory for the probability of this chemical fracture is proposed and confirmed by extensive numerical experiments on a two-dimensional model. This theory follows from the general probability theory of extreme events given by Gumbel. The analytic law differs from the Weibull law commonly used to describe mechanical failures for brittle materials. However, a three-parameter fit with the Weibull law gives good results, confirming the empirical value of this kind of analysis.

Chemical etching of disordered solids is an important technological problem [1], that presents interesting questions in the theory of random systems [2] as well. Strong etching solutions will eventually lead to the fracture of a finite sample, an event defined as “chemical fracture”. In this letter we present a theory for the statistical behavior of this specific fracture mechanism. We show [3] that the deep nature of the *chemical* fracture statistics relies on the probabilistic theory of extreme events due to Gumbel [4]. Interestingly, it is found that our *chemical* fracture statistics are not practically distinguishable from the Weibull statistics empirically introduced to fit *mechanical* fracture statistics [5].

The problem is studied using a simple two-dimensional corrosion picture [6] inspired by an experimental study of pit corrosion of aluminum films [7]. The model describes the chemical etching of a random solid by a finite volume of solution. It predicts that the etching process stops spontaneously on a fractal liquid-solid interface as observed experimentally.

The two-dimensional system is described in fig. 1: The solid is made of lattice sites exhibiting random “resistances to corrosion”  $r_i \in [0, 1]$  uniformly distributed. It has a width  $L$  and a depth  $Y$ . At any time  $t$  the “etching power” of the solution is proportional to the etchant concentration  $C(t)$ :  $p(t) = \Gamma C(t)$ . The solution has a volume  $V$  and contains an initial number  $N_{\text{et}}(0)$  of etchant molecules. Therefore  $p(0) = C(0) = N_{\text{et}}(0)/V$  using  $\Gamma = 1$ . Hereafter we choose  $p(0) > p_c$ , where  $p_c$  is the percolation threshold of the lattice.

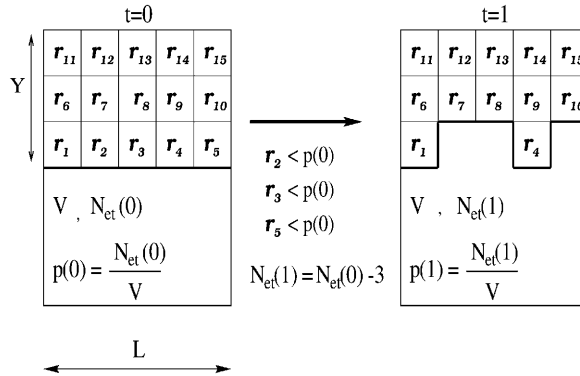


Fig. 1 – Sketch of the etching dynamics in a square lattice: the sites 2,3,5 are etched at the first time-step as their resistances are lower than  $p(0)$ . At the same time the number of etchant particles in the solution decreases by 3 units, and a new part of the solid is uncovered. The process is then iterated.

The solution is initially in contact with the solid through the bottom boundary  $y = 0$ . At each time-step  $t$ , all surface sites with  $r_i < p(t)$  are dissolved and a particle of etchant is consumed for each corroded site. Hence, the solution concentration progressively decreases. For an arbitrarily large sample, the corrosion process always stops spontaneously at a certain time  $t_f$  when the etchant concentration  $p(t_f)$  is still finite [8], reaching a maximal depth  $y_M$ . However, when  $Y$  is finite, the corrosion can reach the bottom of the sample before  $t_f$ , fracturing the solid into two disconnected parts. This “chemical fracture” is a stochastic event which depends on the realization of the random resistances  $r_i$ .

Hereafter we call  $\mathcal{P}(V)$  the fraction of samples broken by a volume  $V$  of solution, keeping the other system parameters  $L$ ,  $p_0$  and  $Y$  fixed. Its measure is shown in fig. 2. The solution

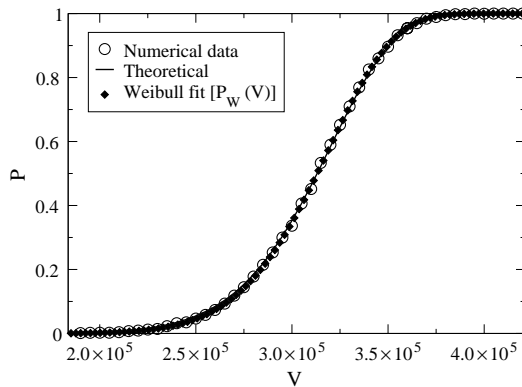


Fig. 2 – Chemical fracture probability  $P(y_M > Y)$  as a function of the volume  $V$  which measures the “chemical force”. Small circles are the numerical estimated probabilities performing 1000 runs for each value of  $V$  applied on a solid of sizes  $L = 1000$  and  $Y = 500$  ( $p_0 = 0.7$ ). Diamonds represent the fit of the fracture data with a Weibull law of parameters  $V_0 = 1.15 \cdot 10^5$ ,  $V_1 = 4.08 \cdot 10^5$ , and  $m = 3.89$ . The line is the result of the fit using eq. (10), as explained in the text (the fitted parameter  $A = 0.3875$ ).

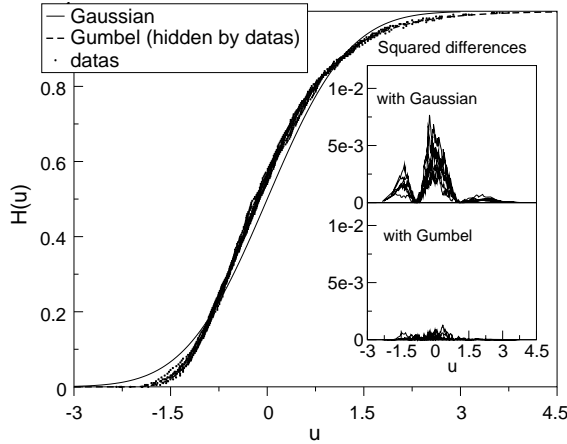


Fig. 3 – The numerical integrated probability distribution for reduced  $y_M$  (zero mean and unitary variance) is compared with standard Gaussian and Gumbel distributions. In the main figure, the simulation results collapse on the Gumbel distribution given by eq. (1) (hidden by data points). In the insets we show the squared difference between data and the Gaussian and Gumbel distributions. The data refer to simulations performed for  $L = 3000, 5000$  and  $N_{\text{et}}(0) = 5 \cdot 10^6, 1 \cdot 10^7, 2 \cdot 10^7, 5 \cdot 10^7$  (1000 different dynamics for each choice of  $L$  and  $V$ ,  $p_0 = 0.7$ ).

volume represents the applied chemical force for given  $p_0$ . Obviously, the fracture event is directly related to the value of the maximal depth  $y_M$  relative to the sample depth  $Y$ : if  $y_M < Y$ , then the fracture does not occur, otherwise the sample will be broken in two distinct pieces. Hence, in order to compute the fracture statistics we have to study the probability distribution of  $y_M$  in a sample with an infinite depth.

Before proceeding, it is important to remark the differences between the *chemical fracture statistics* and the *distribution of the maximal corrosion depth*. The *chemical fracture statistics*  $\mathcal{P}(V)$  is a *parametric* curve which gives the fraction of similar solid samples fractured for a given value of  $V$ . Hence  $\mathcal{P}(V)$  is not a distribution function in the sense of probability theory. In particular,  $V$  is not a random variable but an external parameter.

On the contrary, the *distribution of the maximal corrosion depth* is the probability distribution function (DF) of the random variable  $y_M$ , representing the maximal corrosion depth for an (infinitely deep) sample. This is a genuine probability distribution function and, accordingly, its derivative is the probability density function (pdf) of the variable  $y_M$ . Obviously the two quantities are related, but of a different nature. In the following we will show how it is possible to recover the first, via a probabilistic theory of the second.

The fracture statistics  $\mathcal{P}(V)$  of fig. 2 has been measured numerically taking a sample of a fixed depth and performing several corrosion processes for each value of the solution volume  $V$ , and recording the fraction of broken samples as a function of  $V$  (see fig. 2).

On the other hand, the probability distribution of the maximal corrosion depth has been measured by fixing  $V$  and recording the maximal corrosion depth during several corrosion processes on large systems. A different choice of  $V$  give a different distribution, but a universal scaling form can be recognized. As shown in fig. 3, the numerical DF  $P(z_M < u)$  for the reduced variable  $z_M \equiv (y_M - \langle y_M \rangle) / \Sigma$  (where  $\langle y_M \rangle$  is the average value of  $y_M$  and  $\Sigma$  its standard deviation) is the same for several choices of  $V$ .

Since  $y_M$  is an extremal random variable, we compare this numerical distribution with the

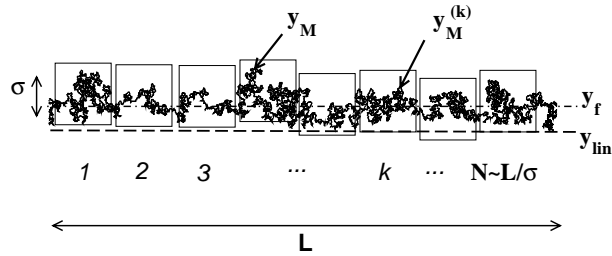


Fig. 4 – Final corrosion front: It is composed of  $N \sim L/\sigma$  independent regions of size  $\sigma$  ( $\sigma$  can be considered as the correlation length of the system). The extremal front position  $y_M$  is indicated. It is the maximum between the  $N$  independent values of  $y_M^{(k)}$  of each region.

standard (*i.e.* with zero mean and unitary variance) Gumbel distribution function  $H(u)$  [4] for extreme events:

$$H(u) = e^{-e^{-(bu+a)}}, \tag{1}$$

where  $a \simeq -0.5772$  and  $b \simeq \sqrt{1.64493}$ .

We recall that the Gumbel distribution is the canonical distribution for the maximal value of a set of random variables in the same manner as the Gaussian distribution is the canonical distribution for the sum. More precisely, if  $\{x_1, \dots, x_N\}$  is a set of independent stochastic variables with identical distribution decaying faster than any power law for large values, then, in the large- $N$  limit, the maximum value among them can be shown to be Gumbel distributed. The collapse of our data on the Gumbel distribution is remarkable, first because there are no adjustable parameters, and second because the points on the interface *are correlated to some extent*.

In the following we discuss why the physics of the etching model determines such a Gumbel behavior. As a second step we will derive from it the theoretical form of  $\mathcal{P}(V)$ . This last task is accomplished considering the probability  $P(y_M > Y)$  and introducing the explicit dependence of  $\langle y_M \rangle$  and  $\Sigma$  on  $V$  (with  $p_0$ ,  $Y$  and  $L$  fixed), *i.e.*

$$\mathcal{P}(V) = 1 - \exp \left[ - \exp \left[ b \frac{\langle y_M \rangle(V) - Y}{\Sigma(V)} - a \right] \right]. \tag{2}$$

Such explicit dependence is obtained using the known scaling results of this particular etching model.

We now proceed with the derivation of the Gumbel law for this etching model. First we have to explain why the corrosion front can be reduced to a set of independent random variables. At the beginning of the dynamics [8],  $p(t)$  follows the exponential law  $p(t) = p_0 \exp[-t/\tau]$  with  $\tau = V/L$ . The corrosion front advances layer by layer up to approximately  $t = t_c$  when  $p(t) = p_c$  and reaches a depth  $y_{lin.} \sim V/L$ . After this period the corrosion front becomes very irregular and finally stops at  $t = t_f$ . At  $t_f$  the etching power  $p_f = p(t_f)$  is slightly smaller than  $p_c$  and the final corrosion front is fractal with dimension  $D_f = 7/4$  up to a characteristic width  $\sigma < L$ . This situation is displayed in fig. 4. As shown in [8], this phenomenon obeys the scaling laws of gradient percolation [9] where the role of the gradient is played by the ratio  $L/V$ . This implies that

- $\sigma \sim (L/V)^{-1/D_f}$ ,
- $\sigma$  can be seen as a percolation correlation length.

The total final corrosion front, shown in fig. 4, can then be considered as a juxtaposition of  $N \sim L/\sigma$  nearly independent fractal boxes of lateral width  $\sim \sigma$  (for a similar recognition of effective independent variables in extreme statistics see [10]). Inside each box  $k$ , there is a point of maximal penetration of the front  $y_M^{(k)}$ . Since such points belong to different boxes, the values  $y_M^{(k)}$  are, by construction, identically distributed and independent random variables. The extreme position of the front is the maximal value between such a collection of random variables. This is why a Gumbel distribution is observed.

More precisely, due to the underlying percolation phenomena, the DF for each  $y_M^{(k)}$  has exponential tail with the same characteristic scale  $\sim \sigma$ :

$$P\left(y_M^{(k)} > y\right) \sim e^{-\frac{y - \langle y_M^{(k)} \rangle}{c\sigma}} \text{ for } y - \langle y_M^{(k)} \rangle > \sigma, \quad (3)$$

where  $c$  is a constant of order 1 (see also some recent results on the size of sub-critical clusters [11]). In this case, the theory of extreme statistics [4] imposes that, for  $N \gg 1$ ,  $y_M$  is asymptotically Gumbel distributed, *i.e.*  $P[(y_M - \langle y_M \rangle)/\Sigma < u] = H(u)$  and that

$$\langle y_M \rangle = \langle y_M^{(k)} \rangle + \Sigma \log N, \quad (4)$$

$$\Sigma = 2c\sigma. \quad (5)$$

It is then necessary to test numerically eqs. (4) and (5) (and specifically the logarithmic dependence on  $N$ , *i.e.* on  $L/\sigma$ ), in order to confirm these arguments. In the situation described in fig. 4 one observes that  $\langle y_M^{(k)} \rangle$  is given by the average depth  $y_f$  of the final corrosion front (average taken over all the final front sites) plus a positive shift of order  $\sigma$ . In turn, the average depth  $y_f$  (a directly measurable quantity in simulations) is given by the depth  $y_{\text{lin.}}$  reached during the linear part of the corrosion in addition to a shift (sub-leading) again of order  $\sigma$ . Therefore from eq. (4) we can write

$$\langle y_M \rangle - y_f \sim \sigma [1 + k_1 \ln(L/\sigma)], \quad (6)$$

$$y_f - y_{\text{lin.}} \sim \sigma, \quad (7)$$

$$y_{\text{lin.}} \sim V/L, \quad (8)$$

$$\Sigma \sim \sigma, \quad (9)$$

where  $k_1$  is a coefficient of order one. Recalling that  $\sigma \sim (V/L)^{4/7}$ , we can substitute  $\langle y_M \rangle$  and  $\Sigma$  as functions of  $V$  in eqs. (5) and (4) in order to obtain the *real* functional dependence of  $\mathcal{P}(V)$  on  $V$  apart from numerical scaling coefficients.

The scaling behaviors are themselves confirmed by the extensive numerical simulations shown in fig. 5. Note that if  $L/\sigma$  is kept constant (*i.e.* if  $L \sim V^{4/11}$ ) then  $[\langle y_M \rangle - y_f] \sim (L/V)^{-1/D_f}$ . The measured exponent  $0.59 \pm 0.02$  is consistent with this prediction. In the same figure, we also report the scaling behavior of the standard deviation  $\Sigma$  and of  $y_f$ . These fits confirm that  $\Sigma \sim \sigma$  and that  $y_f$  can be written as the sum of  $y_{\text{lin.}}$  and a shift of order  $\sigma$ . Finally, the linear logarithmic dependence on  $L$  for fixed  $\sigma$  (*i.e.* for fixed  $L/V$ ), which is the essential confirmation of eq. (4), is shown in the inset. It has also been numerically confirmed that  $\Sigma$  and  $y_f$  does not depend on  $L$  for fixed sigma (not shown in the figure).

To summarize, eq. (2) and eqs. (6)-(9) give the theoretical form for  $\mathcal{P}(V)$ , once the proportionality coefficients in eqs. (6)-(9) and the coefficient  $k_1$  have been determined. For simplicity, it is convenient to rewrite eq. (2) as follows:

$$\mathcal{P}(V) = 1 - \exp \left[ -A \left( \frac{L}{\Sigma} \right)^b \exp \left[ \frac{b(y_f - Y)}{\Sigma} \right] \right]. \quad (10)$$

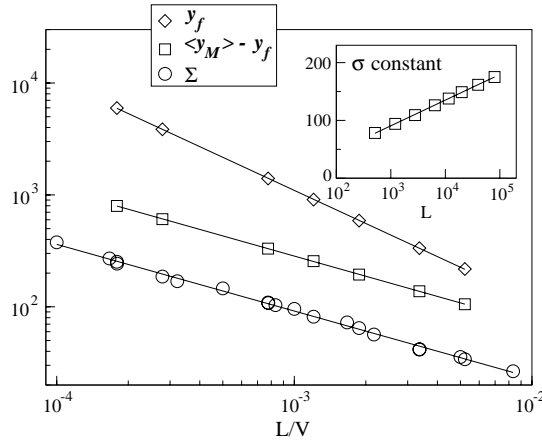


Fig. 5 – Scaling behavior of  $y_f$ ,  $[\langle y_M \rangle - y_f]$  and  $\Sigma$ . The data in the main graph refer to simulations performed with a constant  $L/\sigma$  (range of parameters: from  $L = 522$  and  $V = 5 \cdot 10^8$  to  $L = 11550$  and  $V = 5 \cdot 10^8$ ). The numerical fits are in accordance with the theoretical behaviors. The inset shows the logarithmic dependence of  $\langle y_M \rangle$  on  $L$  for a given  $\sigma$  (parameters range from  $L = 1205$  and  $V = 120500$  to  $L = 80000$  and  $V = 8 \cdot 10^6$ , chosen to have a constant  $\sigma$ ). In both cases the data correspond to 1000 different dynamics for each choice of  $L$  and  $V$ ,  $p_0 = 0.7$ .

The dependence on  $k_1$ , described in eq. (6), is now contained in the coefficient  $A$ . As a closure test of our analysis we choose to use this form to fit against  $A$  the numerical fracture statistics (*i.e.* the fraction of simulation runs breaking the sample as a function of  $V$ ) [12]. As shown in fig. 2, the theoretical form of  $\mathcal{P}(V)$  and the simulation are in excellent agreement.

In summary, we have studied the chemical fracture due to the extremal propagation of a corrosion front in a two-dimensional scalar etching model. It has been shown both theoretically and numerically that the statistics of the maximal depth reached by the solution is given by the well-known Gumbel extremal distribution function. From this it has been possible to extract theoretically the probability of a *chemical fracture*.

Before concluding, we believe that it could be interesting to compare our results with the analysis commonly used for mechanical fracture statistics. In this case, even though a widely accepted theoretical frame is still lacking, the standard empirical fit is often performed using a Weibull law [5]. In our chemical fracture model, this comes to try to fit the data with

$$\mathcal{P}_W(V) = 1 - e^{-\left(\frac{V-V_0}{V_1}\right)^m} \quad \text{with } V > V_0, \quad (11)$$

where  $V_0$  (the minimal stress to have a finite fraction of fractures),  $V_1$  and  $m$  are suitable parameters.

The result, shown in fig. 2, is that the chemical fracture statistics can be fitted very accurately with a Weibull law. We have also verified (not shown here) that the Weibull law probability tails (the test generally used by engineers) fit nicely with our data. On the one hand, we believe that this is astonishing, since, despite the simple scalar nature of the model, we recover, for our purely chemical process, the same empirical statistics found for mechanical failures of brittle materials, generally observed in more complex (vectorial or tensorial) frames. On the other hand, it is important to remark that in the present case the Weibull law is only an empirical fit, because the real analytical form of the chemical fracture statistics is given by eq. (2). Moreover, a Weibull law, which is usually related to the presence of power law

distributed flaws, has no reason to emerge here, as eq. (2) results from a theoretical calculation of the model and directly connected to known results in percolation theory.

As a final remark, one could suggest that the correspondence between the Weibull fit and the underlying Gumbel distribution (first suggested by [13]) found here is linked more generally to gradient percolation. Gradient percolation situations can also be present in solids which *have never been etched* [14]. The essential ingredients of our theory are i) the percolation aspect linked to randomness of the system, and ii) the existence of a gradient. In real systems gradients may exist in the sample, for example the ion concentration gradient in glass fibers used in communication optics. But it may also appear in experiments, for instance in experimental studies of ceramic fracture. In classical flexure experiments the distribution of stress is nonuniform [15]. It remains to be determined specifically if such gradient mechanisms are responsible for some of the ubiquitous apparent Weibull statistics.

Our two-dimensional results could be generalized to higher dimensions, according to [16]. Therein, field-theoretic arguments show that the corrosion dynamics towards the final state can be described as a self-organized absorbing phase transition towards the critical phase of percolation in any dimension.

\* \* \*

We are grateful to M. DEJMEK and S. ZAPPERI for useful comments and we acknowledge the support of the European Community TMR Network ERBFMRXCT980183.

## REFERENCES

- [1] HENCH L. and CLARK J. D., *J. Non-Cryst. Solids*, **28** (1978) 83.
- [2] HERRMANN H. and ROUX S., *Statistical Models for the Fracture of Disordered Media* (North-Holland, Amsterdam) 1990.
- [3] BALDASSARRI A., *Statistics of Extreme Persistent Events*, PhD Thesis, University of Paris XI (1999).
- [4] GUMBEL E. J., *Statistics of Extremes* (Columbia University Press, New York) 1958; GALAMBOS J., *The Asymptotic Theory of Extreme Order Statistics* (R. E. Krieger Publishing Co., Malabar, Flo.) 1987.
- [5] WEIBULL W., *J. Appl. Phys.*, **18** (1951) 293.
- [6] SAPOVAL B., SANTRA S. B. and BARBOUX PH., *Europhys. Lett.*, **41** (1998) 297; SANTRA S. B. and SAPOVAL B., *Physica A*, **266** (1999) 160.
- [7] BALÁZS L., *Phys. Rev. E*, **54** (1996) 1183.
- [8] GABRIELLI A., BALDASSARRI A. and SAPOVAL B., *Phys. Rev. E*, **62** (2000) 3103.
- [9] SAPOVAL B., ROSSO M. and GOUYET J. F., *J. Phys. (Paris) Lett.*, **46** (1985) L149; SAPOVAL B., ROSSO M. and GOUYET J. F., *The Fractal Approach to Heterogeneous Chemistry*, edited by AVNIR D. (John Wiley and Sons Ltd., New York) 1989.
- [10] CURTIN W. A., *Phys. Rev. Lett.*, **80** (1998) 1445.
- [11] BAZANT M. Z., *Phys. Rev. E*, **62** (2000) 1660.
- [12] For  $\Sigma$  and  $y_f$  we impose the scaling predictions eqs. (6)-(9) with coefficients independently fitted from data in fig. 5. From the same data it should be possible to get  $k_1$ , and hence  $A$ . However, the logarithmic nature of the scaling makes this procedure delicate, and we prefer to fit  $A$  instead.
- [13] DUXBURY P. M., LEATHAND P. L. and BEALE P. D., *Phys. Rev. B*, **36** (1987) 367.
- [14] See the breakdown model in ZAPPERI S., HERRMANN H. J. and ROUX S., *Eur. Phys. J. B*, **17** (2000) 131.
- [15] JAYATILAKA A. DE S., *Fracture of Engineering Brittle Materials* (Applied Science Publishers, London) 1979.
- [16] GABRIELLI A., MUNOZ M. A. and SAPOVAL B., *Phys. Rev. E*, **64** (2001) 016108.